Energy Conversion and Management 111 (2016) 125–136

Contents lists available at ScienceDirect

Energy Conversion and Management

journal homepage: www.elsevier.com/locate/enconman

A new Golden Section method-based maximum power point tracking algorithm for photovoltaic systems

A. Kheldoun [a], R. Bradai [b], R. Boukenoui [c], A. Mellit [d,e,*]

[a] Signals and Systems Laboratory, Institute of Electrical and Electronic Engineering, University M'Hamed Bougara of Boumerdes, Avenue of Independence, 35000 Boumerdes, Algeria
[b] LATSI, Faculty of Engineering, University of Blida 1, Department of Electronics, Blida 09000, Algeria
[c] SET Laboratory, Faculty of Engineering, University of Blida 1, Department of Electronics, Blida 09000, Algeria
[d] Renewable Energy Laboratory, University of Jijel, 18000 Jijel, Algeria
[e] The International Centre for Theoretical Physics (ICTP), Starada Costiera, 11-34151 Trieste, Italy

ARTICLE INFO

Article history:
Received 14 August 2015
Accepted 15 December 2015
Available online 6 January 2016

Keywords:
Photovoltaic systems
Maximum power point tracking
Golden-Section Optimization
Steady state oscillations
Partial shading

ABSTRACT

One way to improve the efficiency of solar powered systems is to maximize the energy harvesting from the photovoltaic module by using a maximum power point tracking algorithm. The latter must be simple for implementation, fast and accurate to cope with fast changing atmospheric conditions and partial shading operations. The paper presents a new maximum power point tracking method based on Golde n-Section Optimization technique for photovoltaic systems. The proposed method converges to the Maximum Power Point by interval shrinking. Initially, two points are selected from the search space whose boundaries are known, evaluated then a new point is accordingly generated. At given iteration the algorithm has a new narrowed interval bounded by the new point and one of the initial points according to the evaluation results. The algorithm stops iterating (interval shrinking) when the interval becomes small enough and the photovoltaic system is forced to operate at the average value of the last found interval without perturbing either the voltage or the duty cycle. This makes the photovoltaic system converges rapidly to the maximum power point without voltage or power oscillations around the maximum power point thereby lower energy waste. A comparison results with recently published work are provided to show the validity of the proposed algorithm under fast changing conditions and partial shading.

1. Introduction

The steadily increasing demand on electric energy and rising prices of the fuel used in conventional power plants together with increasing concerns about their environmental effects, have encouraged intensive research for, friendly environmental, low-cost generation plants, particularly solar energy which has proved its worth for power plants of multiple MW proportions, as well as smaller applications such as rural electrifications [1]. Solar energy is considered as one of the most promising renewable energy of the future in Algeria [2] and has become a necessity for people living in the southern to cope with the long hot season [3]. Besides the availability of the sunlight along the year, PV systems are easy to install, present neither moving parts nor combustion processes hence environmentally friendly and almost maintenance free [2]. However, PV systems, which mainly comprise the PVG and power electronic processor, suffer from very low system efficiency, a problem that arguably needs to be addressed. One should differentiate between conversion efficiency and utilisation efficiency of PV modules. Conversion efficiency, being difficult to estimate as a parameter [1], is very low compared to utilisation efficiency which is the ratio of output power to the maximum power that can be extracted at given atmospheric conditions (irradiance, temperature and air mass). In the present work, the latter efficiency is the only parameter of interest. Therefore, one of the most economical ways to improve the utilisation efficiency of PVGs is to ensure that it is always operating at its maximum power point irrespective of the environment conditions. This can be achieved by associating a maximum power point tracking (MPPT) controller to the power electronic converter (usually a chopper) in order to adjust the duty cycle to match the load.

Much work has been devoted to improve the performance of PV systems through developing new or upgrading already existed MPPT algorithms. To this, several papers have been published to

* Corresponding author at: Renewable Energy Laboratory, University of Jijel, 18000 Jijel, Algeria.
E-mail address: adelmellit2013@gmail.com (A. Mellit).

http://dx.doi.org/10.1016/j.enconman.2015.12.039
0196-8904/

Nomenclature

Abbreviation

ACO	ant colony optimization
ANN	Artificial Neural Network
ANFIS	Adaptive Neuro-Fuzzy Inference System
AI	Artificial Intelligence
CS	Cuckoo search
FL	fuzzy logic
GA	Genetic Algorithm
GMPP	global maximum power point
GSO	Golden Section Optimization
HC	Hill Climbing
IC	Incremental Conductance
MPPT	maximum power point tracking
MPP	maximum power point
P&O	Perturb & Observe
PSO	Particle Swarm Optimization
PV	photovoltaic
PVG	photovoltaic generator
PWM	pulse width modulation
STC	Standard Test Conditions

List of symbols

ε	voltage precision
a	diode ideality constant
G	irradiation level in W/m^2
G_{STC}	nominal irradiation level (in 1000 W/m^2)
I	PV array current output
I_{MPP}	current of maximum power point
I_{PV}	light-generated current
I_S	Diode's reverse saturation current
I_{SCN}	nominal short circuit current of the PV module
K	Boltzmann's constant
K_I	short circuit current coefficient
K_V	open circuit voltage coefficient
N_p	number of parallel-connected cells
N_S	number of series-connected cells
q	electron's electric charge
R_{sh}	parallel or shunt resistance
R_s	series resistance
V	PV module's voltage output
V_{OCN}	PV module's nominal open-circuit voltage
V_{MPP}	voltage of maximum power point
V_{PV}	PV array voltage
V_T	thermal voltage of the PV cell
T_{STC}	nominal temperature (298 K)
ΔT	variation from the nominal temperature

review, discuss and classify these MPPT algorithms. For instance, in [4] two main groups of MPPTs are distinguished: conventional group that includes Perturb and Observe (P&O), Incremental Conductance (IC), and Hill Climbing (HC) techniques and stochastic based methods group, then a comparison between those techniques within the same group is done in terms of convergence speed, complexity, ability to truck the true MPP, etc. Different MPPT algorithms which are based on the use of either AI or evolutionary methods have been listed in [5]. A focus has been given to their implementation using FPGA ships and subsequently a comparison between them is made in terms of complexity, efficiency, rapidity and memory space requirement. Classification adopted in [6] is based on the ability of MPPT technique to cope with uniform and non-uniform irradiance. This paper raises the outcome that evolutionary algorithms based MPPT techniques outperform others in terms of seeking GMPP but there are still many concerns when it comes to implementation. A comparison through simulation and implementation using FPGA of four MPPT techniques is presented in [7]. Fuzzy logic, Artificial Neural Network (ANN), Adaptive Neuro-Fuzzy Inference System (ANFIS) and GA-optimized FLC based MPPTs are considered and compared in terms of complexity, rapidity, oscillation around MPP and memory space requirement.

None of the previously mentioned review paper has considered MPPTs which are based on the mathematical model of the PVG. Finding relationship between weather parameters and PVG output voltage and current using either curve fitting or training techniques would make deriving the MPP parameters (duty cycle, current or voltage) an easy forward task. These relationships can be obtained by training an ANFIS to become MPPT controller [8], estimating the input resistance of the PV system (PVG + chopper) which has a direct relationship with MPP [9] or applying nonlinear model identification methods [10]. Model-based MPPT techniques offer the advantage of being very fast but valid only for the PVG under test and cannot cope with partial shading operations.

In general, MPPT algorithms are classified according to the type of the algorithm used. This classification makes difference between conventional methods, Artificial Intelligence techniques (AI) and population-based techniques. Conventional MPPT methods include P&O, IC, HC and their modified version techniques [4]. AI-based MPPT methods use one or combine two of the soft computing techniques: In [11] the authors have designed a fuzzy-logic controller (FLC) for seeking the MPP deliverable by a photovoltaic module using the measured values of the photovoltaic current and voltage. The simulation results show a satisfactory performance with a good agreement between the expected and the obtained values. An adaptive fuzzy logic based MPPT method is proposed in [12]. It consists to integrate two different rules; the first one is used to adjust the duty cycle of the DC–DC converter, while the second one is employed for an online adjusting of the controller's gain. Results indicate that the proposed method outperforms the conventional fuzzy-logic controller. A new embedded digital MPPT system based on ANN is recently developed in [13]. The advantages of the proposed system include low computation requirement, fast tracking speed and high static/dynamic tracking efficiencies. In addition, using the developed neural network model, the photovoltaic generation systems user can apply the developed MPPT controller to any photovoltaic module without the need to modify the firmware of the photovoltaic generation system.

The AI-based MPPT techniques take advantage of the expert's knowledge to develop their control strategy. Population based techniques or evolutionary algorithms are introduced to tackle multivariable optimization problems with multiple optimal points. Some of them have been adapted to deal with MPPT problem. Particle Swarm optimization (PSO) proposed in [14] has been combined with direct duty control to truck the GMPP and eliminate power oscillations at steady state (around MPP). Genetic Algorithm (GA) in [15] has been modified to behave like the conventional P&O by selecting individuals of three chromosomes: voltage, search direction and step size. New individuals are obtained by performing crossover and mutation which integrate the principle of P&O. This results in fast convergence to GMPP. A continuous version of ant colony optimization has been employed to develop a global MPPT in [16] using the archive of solution. As the PSO, ACO has

four parameters which must be well tuned to obtain good search performance, these parameters are: size of solution archive, number of ants in an iteration, convergence speed constant and locality of search space. Cukoo search based MPPT used in [17] is similar to HC/P&O as it uses a step size to generate voltage samples. Beside the use of population instead of single solution, the step size based on Lévy flight offers more randomness to avoid getting trapped by local optima. Unlike PSO and ACO, CS requires tuning of only two parameters.

Conventional MPPT algorithms are mainly simple and easy for implementation. However, the oscillations around the MPP which results in large waste of energy during operation as well as the low performance when the PVG experiences a rapid change in irradiance and temperature are the main drawbacks of the first group [4]. Exceptionally, IC is comparatively more accurate and faster compared to the others algorithms of the same group as it is based on the computation of the gradient. However, at low irradiance, the gradient of the PV characteristics becomes a source of instability and gradient-based algorithms can be trapped by local MPPs in case of non-uniform irradiance or partial shading [4].

The second group of MPPTs, which is based on the use of AI techniques, offers the advantage to be independent of PV model and robust against parameter variations and inputs noises. However, designing such MPPTs require an accurate real-time data or expert knowledge [5]. FL-based MPPT is essentially based on establishing fuzzy rules mapping inputs to the output that can be duty cycle, reference voltage or reference current of the DC–DC converter's PWM controller. Besides, the absence of systematic rules to set up the required number of fuzzy sets for each variable as well as the values of normalization and de-normalization gains, it is very difficult to adjust the overlap membership functions and come up with an accurate fuzzy rules base for the inference system [8]. Both ANN and ANFIS need an input–output mapping data to be used in the training stage except that the ANFIS being designed by optimization requires less computation compared to ANN system [8]. AI-based MPPTs converge rapidly and eliminate the steady state oscillations and can cope with rapid change of climate conditions but are not standard like P&O for instance. In others words, the AI-based MPPT cannot be designed to deal with all PV modules available in the market and fails to converge to the global MPP when the PV module undergoes partial shading [6].

The last group, population based MPPTs, offers in addition to the advantages of the second group, the ability to cope with non-uniform irradiance. In the case of non-uniform irradiance, the P-V characteristic of the PV module exhibits more than one MPP. Thanks to their stochastic search that explores randomly the search space, these algorithms can find the global maximum power point while retaining most of the other advantages. Population-based algorithms use many stochastic parameters such as population size, mutation rate, crossover probability in GA and inertia weight, and weighting factors in PSO. These parameters are randomly chosen and their values must be precisely tuned for the algorithm to converge. In addition, any change in the PV characteristics will affect the performance of the MPPT algorithm and these parameters must be re-adjusted to regain its convergence. Besides, the ability of stochastic MPPTs to converge to the global MPP cannot ensure that the global MPP is reached every time the PV system undergoes partial shading. This can be easily shown by the fact that global search algorithms are mostly used in off line optimization problems and must be run for several times to conclude that the best solution is the global one [18,19].

In this paper, a new and simple maximum power point tracking algorithm is proposed. The algorithm is based on the use of Golden Section Optimization (GSO) technique. In our knowledge, it is the first time that GSO is used to track the MPP under fast changing conditions and partial shading, as proposed in this paper. The search principle of GSO makes it rapidly converging, able to deal with fast variation of the atmospheric parameters and able to converge to the global MPP under partially shaded PV array.

The paper is organized as follows: the mathematical model of PV system is presented in Section 2. In Section 3, the proposed GSO-based MPPT algorithm is described and its application in different real situations is undertaken in Section 4. A conclusion summarizing the advantages of the proposed MPPT algorithm is given in Section 5.

2. PV system modelling

Fig. 1 shows a simplified scheme of a standalone PV system with DC–DC buck converter.

This section is devoted to PV module modelling which is a matrix of elementary cells that are the heart of PV systems. The modelling of PV systems starts from the model of the elementary PV cell that is derived from that of the P–N junction.

2.1. Ideal photovoltaic cell

The PV cell combines the behavior of either voltage or current sources according to the operating point. This behavior can be obtained by connecting a sunlight-sensitive current source with a p–n junction of a semiconductor material being sensitive to sunlight and temperature. The dot-line square in Fig. 2 shows the model of the ideal PV cell. The dc current generated by the PV cell is expressed as follows

$$I = I_{\mathrm{pv,cell}} - I_{s,\mathrm{cell}}\left(e^{\frac{V}{aV_t}} - 1\right) \quad (1)$$

The first term in Eq. (1), that is $I_{\mathrm{pv,cell}}$, is proportional to the irradiance intensity whereas the second term, the diode current, expresses the non-linear relationship between the PV cell current and voltage. A practical PV cell, shown in Fig. 2, includes series and parallel resistances [20]. The series resistance represents the

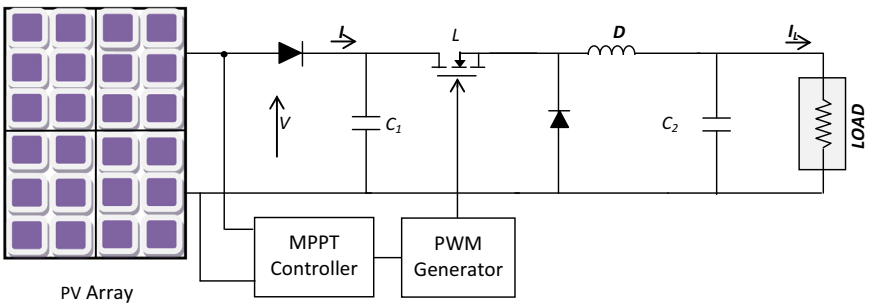

Fig. 1. A PV system with a DC–DC buck converter.

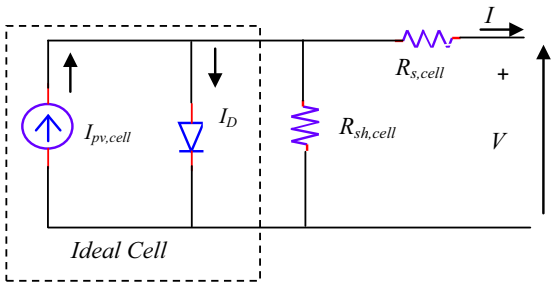

Fig. 2. Equivalent circuit of an ideal and practical PV cell.

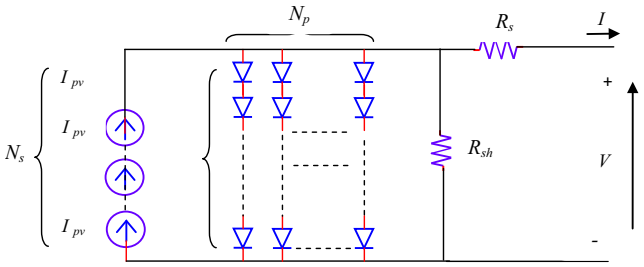

Fig. 3. Equivalent circuit of PV module.

contact resistance of the elements constituting the PV cell while the parallel resistance models the leakage current of the P–N junction.

This model is known as the single diode equivalent circuit of the PV cell. The larger number of diodes the equivalent circuit contains, the more accurate is the modelling of the PV cell behavior, however, at the expense of more computation complexity. The single diode model shown in Fig. 2 is adopted for this study, due to its simplicity.

2.2. PV module modelling

Commercially photovoltaic devices are available as sets of series and/or parallel-connected PV cells combined into one item, the PV module, to produce higher voltage, current and power, as shown in Fig. 3.

The equation of the *I–V* characteristic of the PV module is obtained from Eq. (1) by including the equivalent module series resistance, shunt resistance and the number of cells connected in series and in parallel.

$$I = N_p\left(I_{\text{pv}} - I_s\left(e^{\frac{q(V+I.R_s)}{aN_sKT}} - 1\right)\right) - \frac{(V + I.R_s)}{R_{\text{sh}}} \tag{2}$$

where V_t the PV cell thermal voltage in Eq. (1) is substituted by that of the module thermal voltage given by $V_t = \frac{N_sKT}{q}$ and N_s and N_p are respectively the number of cells connected in series and in parallel forming the PV module.

The constant a expressing the degree of ideality of the diode may be arbitrary chosen from the interval (1, 1.5) [20]. The light generated current of PV cell depends linearly on the irradiance and is also influenced by the temperature:

$$I_{\text{pv}} = \left(\frac{G}{G_{\text{STC}}}\right)(I_{\text{pvn}} + K_i(T - T_{\text{STC}})) \tag{3}$$

I_{pvn} is the nominal light-generated current provided at G_{STC}, T_{STC} which refer to the values at nominal or Standard Test Conditions (1 kW/m^2, 25 °C). The nominal light-generated current is not available in the datasheet of the PV panel but estimated as [20]:

$$I_{\text{pvn}} = \left(\frac{R_s + R_{\text{sh}}}{R_s}\right)I_{\text{scn}} \tag{4}$$

The second term in Eq. (2) is the diode current that is function of the voltage and current coefficients given by the equation below:

$$I_s = \frac{I_{\text{scn}} + K_I\Delta T}{e^{\frac{V_{\text{ocn}}+K_V\Delta T}{aV_t}} - 1} \tag{5}$$

where I_{scn} is the nominal short-circuit current or the maximum current available at the terminals of the practical device at nominal conditions.

Table 1
KC200GT specifications at STC (AM1.5, G = 1 kW/m^2, T = 25 °C).

Parameter	Variable	Value
Peak power (W)	P_{mp}	200.143
Peak power voltage (V)	V_{mp}	26.3
Peak power current (A)	I_{mp}	7.61
Open circuit voltage (V)	V_{ocn}	32.9
Short-circuit current (A)	I_{scn}	8.21
Temperature coefficient of voltage (V/K)	K_v	−0.123
Temperature coefficient of current (A/K)	K_I	0.0032
Number of series cells	N_s	54
Number of parallel cells	N_p	1

2.3. PV module characteristics

The electrical characteristics of the PV module are represented by the *I–V* characteristics for different atmospheric conditions and from which the *P–V* curves are derived. The PV characteristics are the results of solving Eqs. (2)–(5) for different values of PV module voltage, using for example Matlab/Simulink software. Prior simulating the PV module whose parameters are provided by the manufacturer, the identification of the series and parallel resistances must be done. Table 1 reports the specification of the PV module KC200GT at Standard Test Conditions (STC).

Different algorithms of PV parameters extraction are available and the one of [20] can easily be implemented. The algorithm adjusts the values of R_s and R_{sh} so that *I–V* model matches with the three experimental remarkable points (the open circuit point, the short circuit point and the maximum power point).

The remaining parameter that is the ideality factor, a, is adjusted to further improve the model matching with other experimental points others than the remarkable points. Running the algorithm has given the following values: R_s = 0.23 Ω, R_{sh} = 601.34 Ω and a = 1.3. Using the obtained values, Eqs. (2)–(5) are then solved with different irradiance levels and PV cell temperatures. The curve of the PV power can be plotted by multiplying the PV current and PV voltage. Fig. 4(a) shows the PV power versus the voltage with constant temperature (T = 25 °C) varying irradiance G (from 200 to 1000 with step of 200 W/m^2). Fig. 4(b) illustrates the *P–V* characteristics at constant G (1000 W/m^2) but varying cell temperature (10, 30, 50 and 70 °C). It is easy seen from both figures that the MPP locus varies with the variation of the operating climate conditions.

2.4. Partially shaded PV module characteristics

When the PV array operates under uniform solar irradiance, its resulting *P–V* characteristic curve exhibits a single MPP under constant atmospheric conditions as shown in Fig. 4. For the same PV array, the power extracted would not be that shown in Fig. 4, if some parts of the PV array are shaded by a nearby tree, chimney, or cloud. Under partial shading conditions, the shaded region of PV

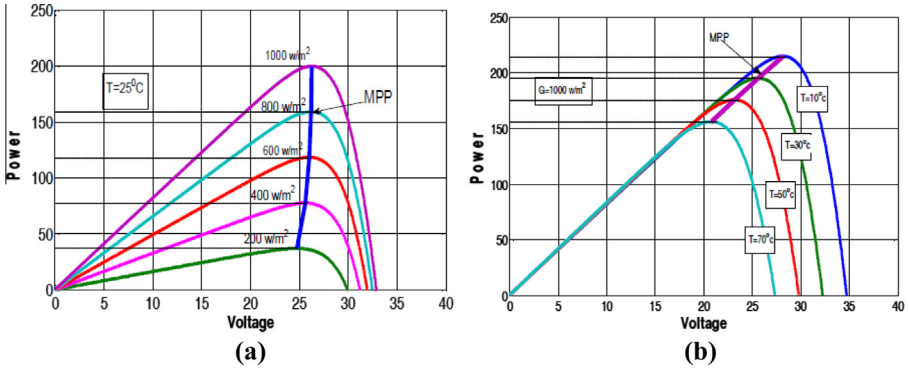

Fig. 4. *P–V* characteristics of KC200GT PV module at different *G* and *T*.

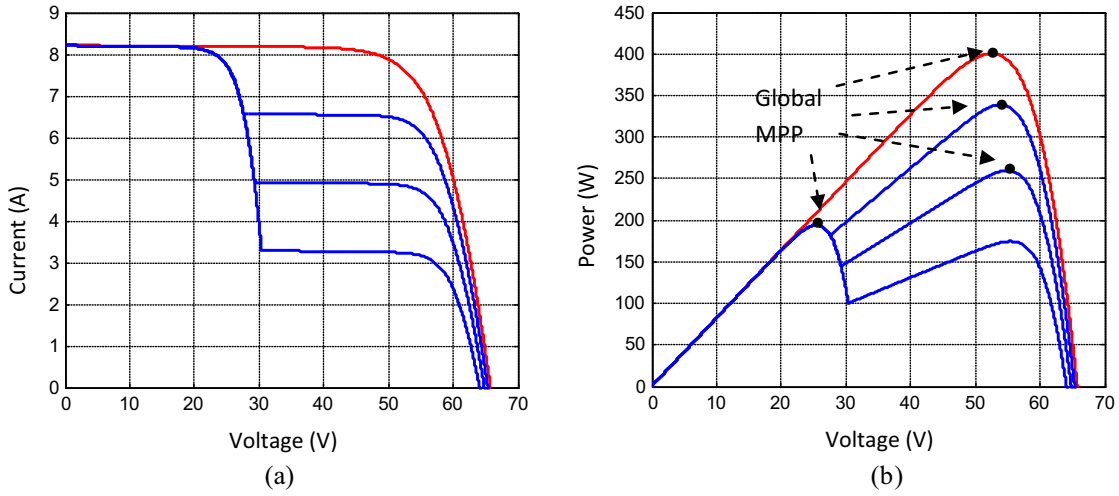

Fig. 5. PV array characteristics under partial shading, (a) *I–V* curve, and (b) *P–V* curve.

receives less intensity of sunlight as compared to other region. The shaded PV module would have to absorb a large amount of the electric power generated by the non-shaded PV modules [6]. This operation condition can damage PV cells of the shaded module. To overcome this problem, a bypass diode is commonly connected in parallel with each PV module in order to provide an alternative path during partial shading, helping to avoid damage of PV modules. However, if the insertion of a bypass diode prevents damaging the PV module it will result in multiple peaks *P–V* characteristics [21].

Fig. 5 depicts *I–V* and *P–V* characteristics of a partially shaded PV array composed of two series connected KC200GT PV modules. The red[1] line represents the characteristic of the PV array with uniform solar irradiance (1 kW/m^2). The blue characteristics are obtained by varying the irradiance of only one module from 0.8 kW/m^2 to 0.4 kW/m^2 with a step of 0.2 kW/m^2.

3. MPPT using Golden Section Optimization technique

The obtained *P–V* characteristics of the KC200GT PV module can be generalized for any commercial PV module in terms of atmospheric parameters effect on the MPP. PV systems must include MPPT controllers to improve the efficiency of the overall system and thereby reducing the payback time.

[1] For interpretation of color in Fig. 5, the reader is referred to the web version of this article.

3.1. Golden Section Optimization (GSO) technique

The name "Golden Section" originates from a classical problem of dividing line segments in a particular way [22–24]. The line segment limited by the search space [*a*, *b*] of length *L* is divided into two sub-segments, the major length L_1 and the minor length L_2, such that

$$\frac{L}{L_1} = \frac{L_1}{L_2} \tag{6}$$

Eq. (6) can be rewritten as

$$\frac{L_1 + L_2}{L_1} = \frac{L_1}{L_2} = \Phi \tag{7}$$

where ϕ is the Golden ratio that is the quotient of the major sub-segment to the minor sub-segment.

Eq. (7) results in following quadratic equation in terms of ϕ:

$$\Phi^2 - \Phi - 1 = 0 \tag{8}$$

Solution of Eq. (8) for ϕ that must be positive results in

$$\Phi = \frac{1+\sqrt{5}}{2} = 1.618 \tag{9}$$

The Golden Section (α) being the ratio of the minor sub-segment and the major sub-segment is the reciprocal of the Golden ratio.

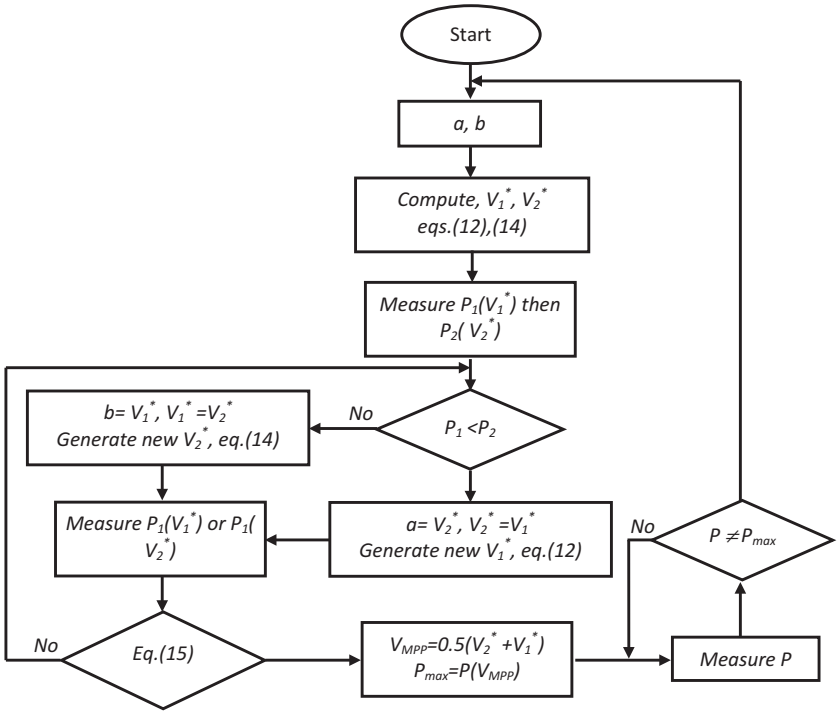

Fig. 6. Flowchart of the Proposed GSO-based MPPT technique.

$$\alpha = \frac{1}{\Phi} = \Phi - 1 = 0.618 \tag{10}$$

In line-search optimization, this method is known as Golden Section Optimization technique that uses the Golden Section to generate two points from the search space (line limited by the interval [a, b]).

$$\begin{aligned} X_1 &= a + 0.618(b-a) \\ X_2 &= b - 0.618(b-a) \end{aligned} \tag{11}$$

The cost function to be maximized, $f(x)$, is evaluated at these two points X_1 and X_2.

- If $f(X_1) < f(X_2)$, the abscissa of the maximum point cannot be less than X_1. Thus, one may conclude that the maximum is in the range of [X_1, b] which is taken as the new interval for the next iteration.
- Else, if $f(X_1) > f(X_2)$, the maximum's abscissa must be less than X_2. Therefore the maximum must lie in the range [a, X_2], the interval taken in the next iteration. The process is continuously repeated until the difference $|X_1 - X_2|$ is less than a certain chosen precision, the resultant maximum's abscissa is given at point $X_0 = 0.5(X_1 + X_2)$.

3.2. GSO-based MPPT

It can be noticed from the previous section that the evaluation needs the knowledge of the cost function, $f(X)$ which is not available in PV system. However, for a given reference voltage, the power is evaluated by measuring first the output PV panel current and voltage, and then multiply the two readings to obtain the power value. Therefore, in GSO-based MPPT system, the searching variable is taken as voltage and the function to be optimized is represented by the P–V curve of the panel that must be on-line sampled. The searching interval could be as [0, V_{ocn}] or slightly reduced from the left since the V_{mp} is always closer to the open circuit voltage. Initially two reference voltage values V_1^*, V_2^* are generated from the starting interval [a, b] such that:

$$V_1^* = a + 0.618(b-a) \tag{12}$$

$$V_2^* = b - 0.618(b-a) \tag{13}$$

The length of the search space is $L = b - a$, therefore upon substituting $b = L + a$ in Eq. (13), the same value of the reference could be written as

$$V_2^* = a + 0.382(b-a) \tag{14}$$

This makes the generation of the two values referred to the same point a. The power values corresponding to these reference voltage values, $P(V_1^*)$ and $P(V_2{}^*)$ are measured then compared and accordingly the search interval is shrunk from either the right or the left. Three points are kept and the forth is taken away. The process is continued until the MPP is reached, that is

$$\left|V_2^* - V_1^*\right| \leqslant \varepsilon \tag{15}$$

Once the MPP is reached, the voltage reference is kept constant by the PI controller and the system is forced to operate at that point, unless a change in T or G occurs and the algorithm restarts the search of the new MPP. The flowchart depicted in Fig. 6 summarizes the entire proposed algorithm.

4. Results and discussion

To verify the effectiveness of the proposed algorithm different simulations have been carried out using MATLAB/Simulink software and under different conditions namely: STC conditions, fast varying atmospheric conditions and under partial conditions.

Fig. 7 shows the MATLAB/Simulink program of the whole system shown in Fig. 1. The flowchart of the GSO-based MPPT depicted in Fig. 6, implemented using embedded function available in the software's library. Both the PV module and the buck converter being used as interface between the load and the PV

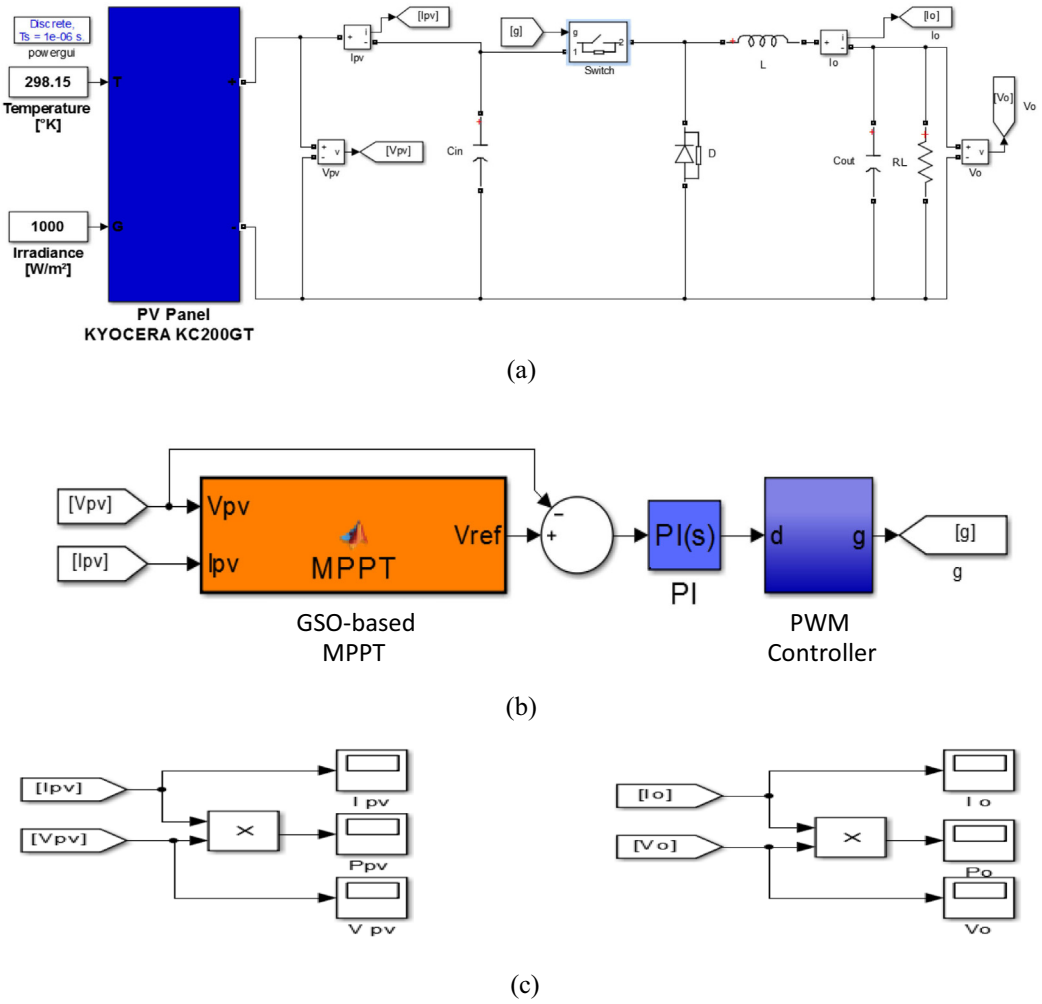

Fig. 7. MATLAB/Simulink program of the developed GSO-based MPPT system: (a) PVG + buck DC–DC converter, (b) control circuit (GSO-MPPT + PI + PWM circuit) and (c) measurements.

Table 2
Values of components of the DC–DC converter.

Components	Values
Load resistor, (R_L)	1 Ω
Inductor, (L)	300 μH
Input capacitor, (C_{in})	100 μF
Output capacitor, (C_{out})	990 μF
MOSFEt's switching frequency, (f_s)	100 kHz

generator is implemented using '*SimPowerSystems*' toolbox, available also in the same software. The parameters of the buck DC–DC converter components are listed in Table 2.

4.1. Test under STC

Under Standard Test Conditions (STC) the PV module exhibits the same atmospheric conditions shown in the datasheet provided by the manufacturer which are $G = 1000\ W/m^2$, $T = 25\ °C$. The simulation starts with a random operating point that is different from the maximum power operating point (V_{mp}, I_{mp}) and the initial maximum power chosen in the GSO-based MPPT is zero. This makes the algorithm starts seeking the real P_{mp}. Fig. 8 depicts the variation of the reference voltage generated by the GSO-based MPPT algorithm, the PV voltage and the output or the load voltage. Fig. 9 illustrates the waveforms of the PV module current and the load current and the power extracted from the PV module. The process of shrinking the interval is clear in the curve of the reference voltage. The algorithm has made 7 iterations to reach the desired voltage or $V_{mp} = 26.3\ V$ according to the datasheet.

From Fig. 8(b), it can be noticed, that once the algorithm converged to the MPP, the voltage of the PV module as well as the load voltage (chopper's output voltage) are maintained constant without any oscillations. The time response to reach the steady state operating point is about 0.02 s. The current of PV as well as the output current go through the dynamic of the same time to settle down to their maximum power values, as shown in Fig. 9(a).

The steady state output power of the PV is 200 W, Fig. 9(b), which is the maximum power that can be extracted from the panel at $G = 1000\ W/m^2$. When the GSO-based MPPT algorithm seeks, the optimal voltage causes oscillations of PV voltage and current during P_{mp} search. These oscillations of current and voltage result in power oscillations and take only 0.025 s, which is the convergence time of the algorithm.

4.2. Test under variable irradiance

In this test, the temperature is kept constant at $T = 25\ °C$ and different step changes in the irradiance are introduced. The time step of irradiance change is set to 0.2 s that is a perturbation

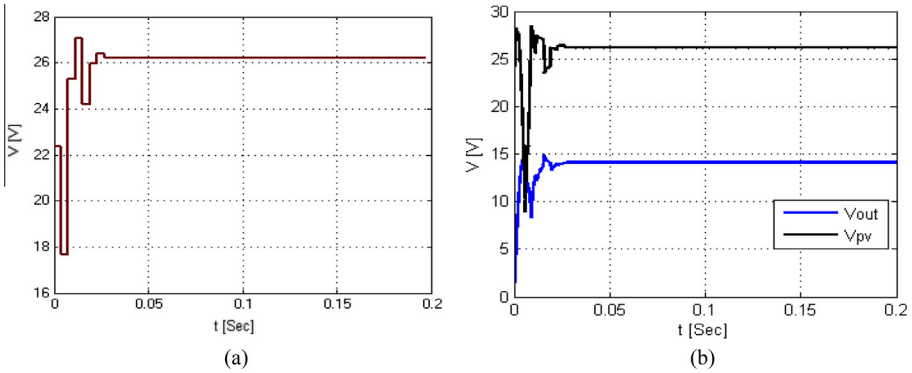

Fig. 8. MPP's seeking process by GSO-based MPPT: (a) reference voltage, and (b) PV and load voltages.

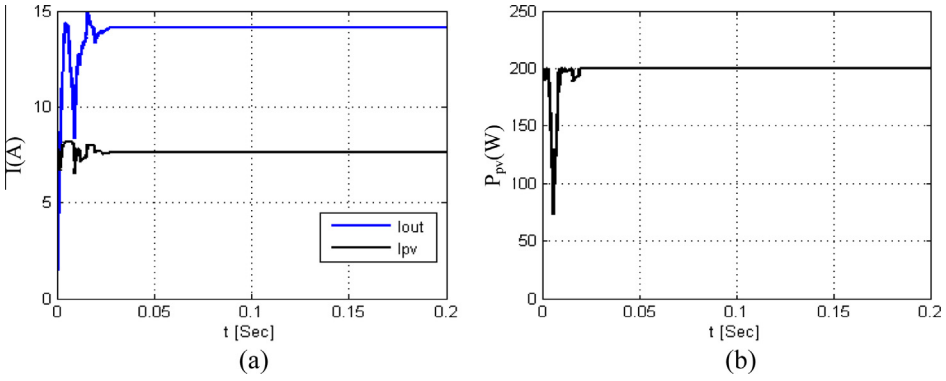

Fig. 9. MPP tracking: (a) current waveforms, and (b) PV panel output power.

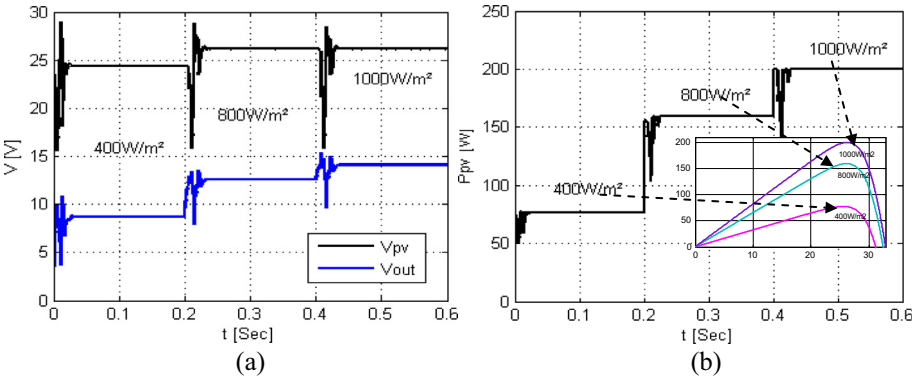

Fig. 10. Results of changing in the irradiance level: (a) voltage waveforms, and (b) PV panel output power.

frequency of 5 Hz. The initial irradiance is $G = 400\ W/m^2$, then stepped up to $G = 800\ W/m^2$, and finally increased to $G = 1000\ W/m^2$. The obtained results are shown in Fig. 10.

Using the *P–V* characteristics of the PV module under study, it is easy to check the matching between the maximum power points corresponding to the different irradiance levels and those obtained by the GSO-based MPPT algorithm. Besides, oscillations of voltage do not exist at all which results in constant output power of the PV panel and thereby avoiding waste of energy due to oscillations. Except the oscillations due the Golden-section search, the output power is almost very close to the maximum power produced by the PV module.

4.3. Test under variable temperature

In this test, the irradiance is kept constant at $G = 1000\ W/m^2$ and a sequence of step change in temperature is introduced. The time step of temperature change is the same as that of the irradiance, 0.2 s (or $f_{MPP} = 5$ Hz). The temperature starts with 25 °C stepped up to 50 °C and finally to 70 °C. The obtained results are depicted in Fig. 11. Upon comparison of the *P–V* characteristics at the above temperature values with those extracted by GSO-based MPPT algorithm, the effectiveness of the latter and its accuracy in tracking the maximum power when the PV panel undertakes variation of temperature can be checked.

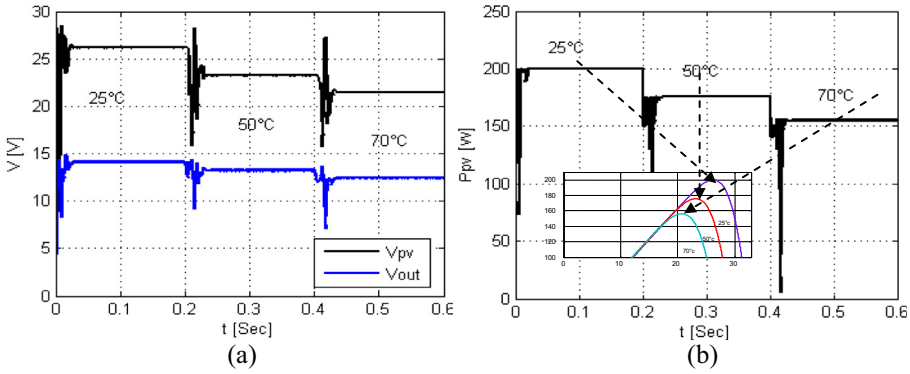

Fig. 11. Results of changing the temperature: (a) voltage waveforms, and (b) PV panel output power.

4.4. Tests under partial shading

In this subsection, the behavior of the proposed algorithm is investigated while the PV module undergoes partial shading. Two tests have been carried out on the PV array, whose *P–V* characteristics are shown in Fig. 5.

4.4.1. Test 1

Initially, the PV array is operated under uniform condition $T = 25\ ^{\circ}C$, $G = 1000\ W/m^2$. At $t = 0.2$ s the partial shading occurs when the irradiance of one module is reduced to $800\ W/m^2$ such that the resulting *P–V* characteristic curve is the one given on Fig. 5(b) and the maximum power available is 340 W. Fig. 12 shows the simulation results of the PV array under these conditions by using the developed GSO-based MPPT algorithm. Under uniform irradiance and standard temperature, the PV array generates 400 W along the interval from 0 to 0.2 s, see Fig. 12(b). This value is the result of the sum of two identical series connected PV modules operating at their maximum power point thanks to the GSO-based MPPT.

At $t = 0.2$ s, one of the modules receives an irradiance of $800\ W/m^2$ which makes the PV panel undergoes partial shading and the *P–V* characteristic of the PV has two peaks with the global MPP being 340 W. Fig. 12(a) and (b) shows that the proposed algorithm converged rapidly to the appropriate voltage leading to the MPP of 340 W.

4.4.2. Test 2

To assess the robustness of the proposed algorithm in seeking the global MPP, the PV array has been subjected to non-uniform irradiance from the starting. PV module 1 receives an irradiance of $800\ W/m^2$ and the other one receives $1000\ W/m^2$, the temperature is kept constant at 25 °C. The obtained results are shown in Fig. 13. It is clearly observed, that the GSO-based MPPT is not trapped by the local maximum power of the *P–V* characteristics and has converged accurately to the global MPP. The way the algorithm seeks the appropriate voltage looks like that used by evolutionary algorithms which are global search algorithms such as Particle Swarm Optimization algorithm. In fact, initial population or particles are chosen in such a way some of them are located in the current source-like region curve, some are chosen from the voltage source-like region curve and the remaining are chosen between the two regions [14]. After the evaluation, new particles will be generated using the concept of the velocity, the personal best particle and the global best particle. At the end, all particles will converge to the global best particle and their velocities will be closer to zero.

4.5. Comparison with other methods

In this section, a performance comparison between the proposed method and others recently published MPPTs is undertaken. To this, different indices are adopted and employed in order evaluate the performances of the proposed MPPT method. Some MPPT techniques are validated under static tracking condition only and some of them have been validated even under dynamic tracking conditions. Because of this, two different comparison studies will be investigated in this section. The first study, which regards static tracking, compares the proposed MPPT with others based on some performances indices such as: response time, static error, algorithm's complexity, required sensors, sensitivity, tracking efficiency among others. The second study, which regards dynamic tracking, compares the proposed the MPPT with others based on the dynamic efficiency, convergence time and complexity level.

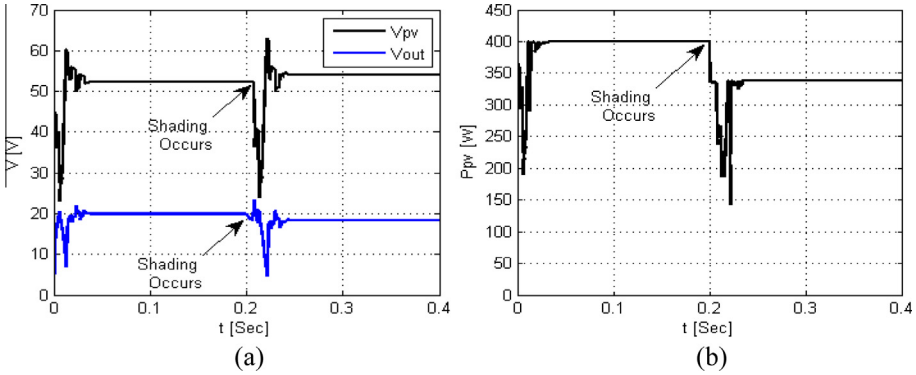

Fig. 12. Operation under partial shading, (a) voltage waveforms, and (b) PV panel output power.

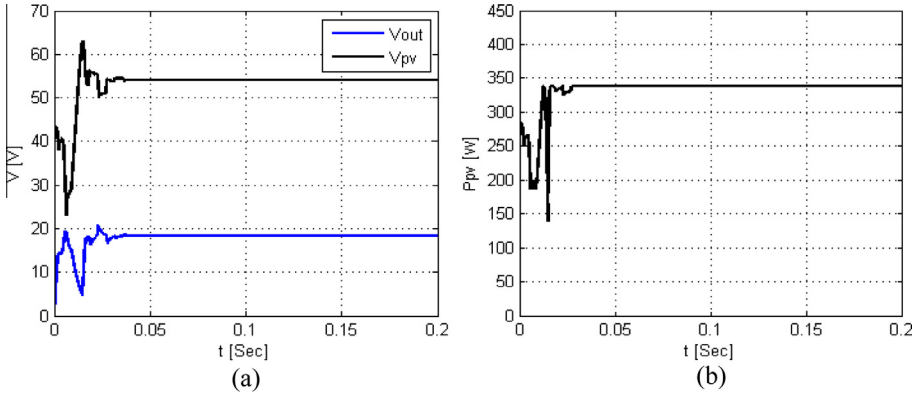

Fig. 13. Operation under partial shading, test 2 (a) voltage waveforms, and (b) PV panel output power.

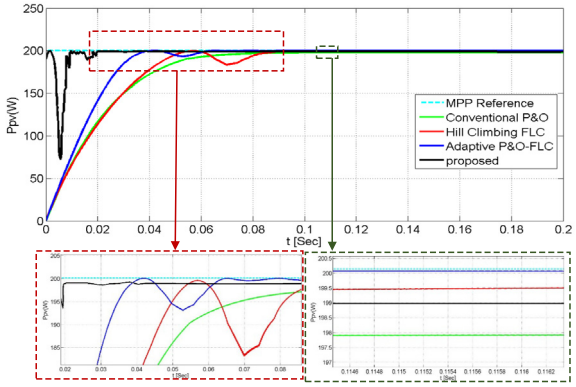

Fig. 14. The PV output power of the compared methods at STD.

4.5.1. Regarding static tracking

In this test, the proposed method is compared with the conventional P&O MPPT method and two recently published MPPT algorithms which are based on fuzzy logic control. The fuzzy logic based MPPT [25] was called Hill-Climbing FLC. This technique uses 16 fuzzy control rules which have been derived from the principle of conventional Hill-Climbing MPPT technique. Therefore, this technique aims to take advantage of the Hill-Climbing search and overcome its three drawbacks, such as: the slow convergence, the considerable steady state oscillations and the large deviation from the MPP under fast variations of irradiance level. The second MPPT is known as adaptive P&O-FLC method [26]. This method is inspired from the principle of the conventional P&O MPPT algorithm. This method uses the same inputs of conventional P&O and replaces the comparison, switching and duty cycle updating by fuzzy logic controller. The universe of discourse of the two inputs has been covered by 5 fuzzy sets which results in 25 fuzzy rules.

In this work, the two above methods have been reprogrammed using Matlab/Simulink software package and applied to the same PV module associated with GSO-MPPT controller being proposed in this work.

Fig. 14 shows the simulation results of the above two MPPT techniques, the conventional P&O MPPT and the GSO-MPPT. Simulation has been done at STC in order to compute the static efficiency that is the ratio of steady state power output to the P_{mpp} provided by the PV module's manufacturer. It can be noticed that all the MPPT techniques have converged to the right MPP but with different performance indices that are shown in Table 3.

It can be observed that conventional P&O method has low complexity but it presents the highest static error (2.343 W) and the lowest efficiency (98.83%). It is obvious that Hill-Climbing FLC presents less complexity with only 16 rules as compared to the adaptive P&O-FLC and outperforms the conventional P&O. However, the static efficiency is lower as compared to that of the adaptive P&O-FLC that provides the highest static efficiency but at the expense of using 25 rules making it the most complex in terms of implementation.

The proposed method performs better control in terms of convergence time and presents an algorithm as simple as that of the P&O. In addition, the proposed method does not require knowledge about the PV system and uses only two sensors. The static error of the proposed GSO-MPPT is higher than those presented above but lower than that of the conventional P&O MPPT that is still used.

4.5.2. Regarding dynamic tracking

In the previous section, it has been shown that the proposed GSO-MPPT tracks accurately the MPP irrespective of the climate conditions. In fact, to verify the dynamic tracking of the proposed algorithm, the PV module must exhibits a special variation of the irradiance according to the European Standard EN50530 [27].

The test sequence starts with 30% of G_{STC} that takes some initial setting time, and then the irradiance is linearly increased with a given slope during a raise time t_1 to standard G_{STC}. The irradiance

Table 3
Performances of the four MPPT methods.

Evaluated parameters	Proposed method	Conventional P&O	Hill Climbing FLC	Adaptive P&O-FLC
Response time (s)	0.025	0.069	0.055	0.04
Static error (W)	1.143	2.343	0.643	Negligible
Power production (W)	199	197.8	199.5	200.1
Static efficiency (%)	99.43	98.83	99.68	99.98
Sensors used	(Current, voltage)	(Current, voltage)	(Current, voltage)	(Current, voltage)
Tracking method	GSO	P&O	FLC with 16 rules	FLC with 25 rules
Algorithm complexity	Very low	Very low	Medium	High
Direct duty cycle control	No	No	Yes	Yes
Robustness	Yes	Yes	Yes	Yes

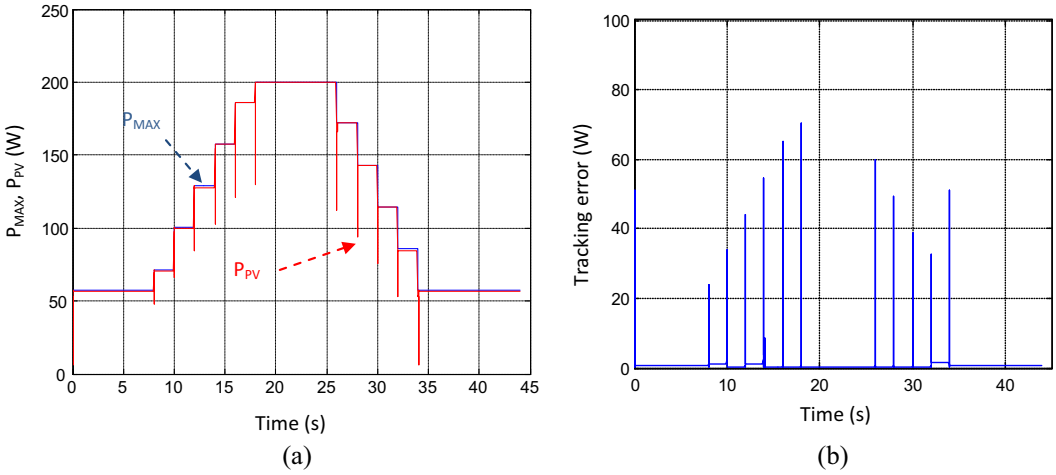

Fig. 15. Dynamic tracking results: (a) power waveforms, and (b) tracking error.

is kept constant during a period of time t_2 (dwell time of the high irradiance level) then linearly dropped to its initial value for a period of time t_3 after which the irradiance will be kept constant lasting t_4 (dwell time of the low irradiance level). This pattern is repeated as much as required by the different tests. Once the test is over, the dynamic tracking efficiency is calculated as follows:

$$\eta_{\text{dynamic}} = \frac{\int_0^T V \cdot Idt}{\int_0^T P_{\text{MAX}} dt} \cdot 100 = \frac{\int_0^{44} P_{\text{pv}} dt}{\int_0^{44} P_{\text{MAX}} dt} \cdot 100 \quad (16)$$

The first pattern test of the European Standard has been chosen with little modification to avoid obtaining a symmetric variation profile of the irradiance and therefore increasing the degree of difficulty. Fig. 15 depicts the simulated tracking waveforms and the tracking error respectively. The peaks of P_{pv} in Fig. 15(a) that result each time the irradiance level is changed come from the fact that GSO-based MPPT generates two voltage references from the search space (from the left and from the right). It is obvious that one is closer to the MPP but other is far from it. Therefore, the later causes the biggest peak. After that, power peaks decline as the search space around the MPP narrows till the algorithm converges to the real MPP. To compute the dynamic efficiency, Matlab built-in function "*trapz*" has been used to approximate the two integrals in the nominator and the denominator of Eq. (16). The dynamic efficiency has been found to be 99.602%.

Table 4 depicts a comparison in terms of dynamic tracking efficiency and convergence time between the GSO-MPPT and the two EML-based MPPTs proposed in [9]. As can be seen from Table 4, the dynamic efficiency of the proposed GSO-based MPPT is comparable with the efficiency of the methods [9] but the convergence to MPP is slower. Obviously, EML-based MPPTs are very fast because both methods piecewise line segments (PLS) and cubic equation (CE) use an emulator of MPP locus (EML). Using either a PLS or CE to model the MPP locus makes the process of seeking the MPP as simple as a forward computation of first order or polynomial single variable equation respectively.

The parameters of these equations are obtained by an off-line trained ANN using the PV characteristics of the investigated PVG. As results, both MPPT methods are model-based techniques that are expected to be very fast. However, besides the lack of robustness of model-based MPPTs, both techniques [13] are trained using data obtained by varying only the irradiance level. To take into account the effect of the temperature, a compensation circuit is used to shift left/right if the operating temperature increases/decreases, however, shifting the operating point is not as accurate as seeking the MPP using an MPPT algorithm. As reported in [5], the main drawback of ANNs or ANFIS-based MPPT is that it could fail when the PV modules start to be degraded, in this situation, training with new data should be carried out periodically. Finally, upon comparison with the aforementioned methods, the proposed GSO-based MPPT's can easily track the global MPPT with fast convergence time.

Table 4
Dynamic tracking efficiency and complexity level.

MPPT method	η_{dynamic} (%)	Convergence time (s)	Complexity level
PLS [13]	99.67	0.007	Medium
CE [13]	99.85	0.007	Medium
ANFIS [8]	–	0.25	Medium
GSO (proposed)	99.602	0.025	Easy

5. Conclusion and future work

In order to improve the efficiency of PV systems, the PV module is associated to a chopper whose voltage or duty cycle is controlled by a MPPT algorithm. In this paper, a new MPPT algorithm which is based on Golden Section Optimization technique is proposed. First, the paper presents the principle of the Golden Section Optimization technique and then derives the flowchart of the MPPT based on this new investigated technique. Several tests have been conducted to verify the performances of the algorithm under STC conditions, fast changing conditions and partial shading operations. The main advantages are:

1. Only addition/subtraction and multiplications are used in the algorithm which employs a few arithmetic operations to compute the reference voltage.
2. The convergence of the algorithm is very fast as the MPP is reached approximately within seven (7) steps.
3. Once the MPP is reached, the PV module operates with constant voltage and current without any steady state oscillations avoiding hence waste of energy due to oscillations.
4. Under fast changing atmospheric conditions, the algorithm exhibits high dynamic efficiency with very low tracking error.
5. Finally under partial shading condition, the proposed MPPT technique behaves like a global search algorithm and efficiently tracks the global MPP.

Besides, the algorithm has no parameter to tune and needs only the knowledge of the value of the open-circuit voltage of the PV

module under study. This value constitutes the upper value while zero is the lower value of the search space used by the GSO-based MPPT.

Experimental prototype of the deigned GSO-based MPPT (e.g. implementation into a low cost microcontroller) for real time applications will be the subject of out further investigations.

Acknowledgement

Dr. A. Mellit expresses a special acknowledgment to the International Centre for Theoretical Physics (ICTP), Trieste, Italy.

References

[1] Kazmerski Lawrance L. Photovoltaics: a review of cell and module technologies. Renew Sustain Energy Rev 1997;1:71–170.
[2] Zafar S. Renewable energy in Algeria, December 23, 2013, <http://www.ecomena.org/renewables-algeria/>. 2013.
[3] Hadj Ammar MA, Benhaoua B, Balghouthi M. Simulation of tubular adsorber for adsorption refrigeration system powered by solar energy in sub-Sahara region of Algeria. Energy Convers Manage 2015;106:31–40.
[4] Kamarzaman NA, Tan CW. A comprehensive review of maximum power point tracking algorithms for photovoltaic systems. Renew Sustain Energy Rev 2014;37:585–98.
[5] Mellit A, Kalogirou SA. MPPT-based artificial intelligence techniques for photovoltaic systems and its implementation into field programmable gate array chips: Review of current status and future perspectives. Energy 2014;70:1–21.
[6] Ishaque K, Salam Z. A review of maximum power point tracking techniques of PV system for uniform insolation and partial shading condition. Renew Sustain Energy Rev 2013;19:475–88.
[7] Chekired F, Mellit A, Kalogirou S, Larbes C. Intelligent maximum power point trackers for photovoltaic applications using FPGA chip: a comparative study. Sol Energy 2014;101:83–99.
[8] Kharb RK, Shimi S, Chatterji S, Ansari MF. Modeling of solar PV module and maximum power point tracking using ANFIS. Renew Sustain Energy Rev 2014;33:602–12.
[9] Li Shaowu. A maximum power point tracking method with variable weather parameters based on input resistance for photovoltaic system. Energy Convers Manage 2015;106:290–9.
[10] Tsang KM, Chan WL. Model based rapid maximum power point tracking for photovoltaic systems. Energy Convers Manage 2013;70:83–9.
[11] Messai A, Mellit A, Massi Pavan A, Guessoum A, Mekki H. FPGA-based implementation of a fuzzy controller (MPPT) for photovoltaic module. Energy Convers Manage 2011;52:2695–704.
[12] Guenounou O, Dahhou B, Chabour F. Adaptive fuzzy controller based MPPT for photovoltaic systems. Energy Convers Manage 2014;78:843–50.
[13] Liu Y-H, Liu C-L, Huang J-W, Chen J-H. Neural-network-based maximum power point tracking methods for photovoltaic systems operating under fast changing environments. Sol Energy 2013;89:42–53.
[14] Ishaque K, Salam Z, Amjad M, Mekhilef S. An improved particle swarm optimization (PSO)-based MPPT for PV with reduced steady-state oscillation. IEEE Trans Power Electron 2012;27:3627–38.
[15] Daraban S, Petreus D, Morel C. A novel MPPT (maximum power point tracking) algorithm based on a modified genetic algorithm specialized on tracking the global maximum power point in photovoltaic systems affected by partial shading. Energy 2014;74:374–88.
[16] Jiang LL, Maskell DL, Patra JC. A novel ant colony optimization-based maximum power point tracking for photovoltaic systems under partially shaded conditions. Energy Build 2013;58:227–36.
[17] Ahmed J, Salam Z. A maximum power point tracking (MPPT) for PV system using Cuckoo search with partial shading capability. Appl Energy 2014;119:118–30.
[18] Panda S, Swain S, Rautray P, Malik R, Panda G. Design and analysis of SSSC-based supplementary damping controller. Simul Model Practice Theory 2010;18:1199–213.
[19] Rajabioun R. Cuckoo optimization algorithm. Appl Soft Comput 2011;11:5508–18.
[20] Villalva MG, Gazoli JR. Comprehensive approach to modeling and simulation of photovoltaic arrays. IEEE Trans Power Electron 2009;24:1198–208.
[21] Ishaque K, Salam Z. A comprehensive MATLAB Simulink PV system simulator with partial shading capability based on two-diode model. Sol Energy 2011;85:2217–27.
[22] Yang WY, Cao W, Chung T-S, Morris J. Applied numerical methods using MATLAB. John Wiley & Sons; 2005.
[23] Ta C-M, Hori Y. Convergence improvement of efficiency-optimization control of induction motor drives. IEEE Trans Ind Appl 2001;37:1746–53.
[24] Lu Y. A golden section approach to optimization of automotive friction materials. J Mater Sci 2003;38:1081–5.
[25] Alajmi BN, Ahmed KH, Finney SJ, Williams BW. Fuzzy logic-control approach of a modified hill-climbing method for maximum power point in microgrid standalone photovoltaic system". IEEE Trans Power Electron 2011;26:1022–30.
[26] Atiqi Mohd Zainuri MA, Mohd Radzi MA, Soh Azura Che, Abd Rahim N. Development of adaptive perturb and observe-fuzzy control maximum power point tracking for photovoltaic boost dc – dc converter. Renew Power Gener IET 2014;8(2):183–94.
[27] E. 50530. Overall efficiency of grid connected photovoltaic inverters; 2010.